JOURNAL OF MOLECULAR SPECTROSCOPY **118,** 103–120 (1986)

Rotational Spectroscopy of DO_2 by FIR LMR and Millimeter-Wave Absorption

TREVOR J. SEARS

Department of Chemistry, Brookhaven National Laboratory, Upton, New York 11973

GERALD A. TAKACS[1] AND CARLETON J. HOWARD

Aeronomy Laboratory, NOAA, Environmental Research Laboratories, 325 Broadway, Boulder, Colorado 80303

AND

RICHARD L. CROWNOVER, PAUL HELMINGER,[2] AND FRANK C. DE LUCIA

Department of Physics, Duke University, Durham, North Carolina 27706

We report the measurement of approximately 50 rotational transitions in the DO_2 radical between 230 and 2530 GHz by high-resolution millimeter-wave and far-infrared laser magnetic resonance spectroscopy. The radical was generated in the gas phase by the reaction of chlorine atoms and oxygen or discharged oxygen with deuterated methanol. The data were analyzed in conjunction with previously published high-resolution spectra of the molecule in the ground vibronic state in order to extract the best set of parameters in the effective Hamiltonian describing the molecule. The fine structure (spin–rotation) parameters derived in the present work were used together with those for HO_2 [A. Charo and F. C. De Lucia, *J. Mol. Spectrosc.* **94,** 426–436 (1982)] in order to determine all of the symmetry-allowed spin–rotation tensor components for the hydroperoxyl radical. The results cannot be interpreted in terms of contamination of the ground state wavefunction by the lowest lying $\tilde{A}^2A'$ state alone and information from quantum chemical calculations of spin–orbit matrix elements between the ground and higher excited states or additional experimental data involving higher excited electronic states are necessary before a complete rationalization of the results is possible.

INTRODUCTION

The hydroperoxyl radical, HO_2, is an important intermediate in the combustion of hydrocarbons and in atmospheric chemistry; however, high-resolution spectra in the gas phase were only observed quite recently when Evenson and co-workers (*1, 2*) detected rotational transitions in the molecule by far-infrared laser magnetic resonance (FIR LMR) spectroscopy. Apart from its chemical importance, the molecule is spectroscopically interesting as a prototypical light asymmetric-top free radical; a series of high-resolution studies (*3–7*) have investigated the molecule's structure in its ground

[1] NOAA–NRC Senior Research Associate, 1982–1983, on leave from Department of Chemistry, Rochester Institute of Technology, Rochester, N.Y. 14623.

[2] Permanent address: Department of Physics, University of Southern Alabama, Mobile, Ala. 36688.

0022-2852/86 $3.00

electronic state. The deuterated species, DO_2, has also been the subject of several studies by microwave spectroscopy (*8, 9*) and EPR and FIR LMR (*10*). Taken together, the spectroscopic data for the two isotopes have established an accurate r_0 structure (*10*) and details of the electronic structure such as the spin–rotation (*11, 12*) and dipolar magnetic hyperfine coupling tensor components (*9*).

Following these spectroscopic studies, several investigators have used the same techniques to measure the kinetics of some reactions involving the hydroperoxyl radical which are of interest in atmospheric and combustion chemistry (*13*). Parallel studies of DO_2 are useful in the understanding of the details of the reaction mechanisms such as the deuterium isotope effect and collision complex dynamics. The desire to perform such experiments led to the present work. Although the FIR LMR spectrum of the DO_2 radical has been studied by Barnes *et al.* (*10*), the spectra measured were at longer wavelengths than those available with the water vapor laser LMR spectrometer on which the kinetic measurements were to be made. We therefore recorded the DO_2 spectrum on the 118.6-μm water vapor laser line. At this wavelength, the rotational transitions observed involve higher rotational levels than had previously been studied and it was found that the best available set of molecular parameters (*9*) did not accurately reproduce the observed spectrum. In an attempt to obtain a reliable description of the molecular rotational energy level structure, the new data were combined with the previously reported high-resolution data (*9, 10*) involving the ground state of DO_2 in a fit to the effective Hamiltonian for this state of the molecule. While this process was reasonably successful, allowing assignment of the new data, it was not possible to determine all of the expected fine structure parameters reliably. Specifically, the off-diagonal component of the spin–rotation tensor $|\tilde{\epsilon}_{ab} + \tilde{\epsilon}_{ba}|$ (*11*) was not well determined; in fact the addition of the new LMR data appeared to confuse the situation and the resulting molecular parameters were, in some cases, more poorly determined than had previously been the case (*9*).

At this stage, it was decided that additional high-precision measurements recorded in the absence of the magnetic field used in the LMR experiment were needed if the effective spin–rotation Hamiltonian parameters were to be determined sufficiently precisely. For this reason, we have recorded more than 40 new rotational transitions at frequencies between 230 and 420 GHz. The available rotational spectra of DO_2 now include information on levels with $N \leqslant 22$ and $K_a \leqslant 4$. A least-squares fit to a representative sample of the data allows the determination of all of the major parameters appearing in the effective Hamiltonian including all of the determinable components of the spin–rotation tensor. These are combined with the corresponding parameters for HO_2 (*6*) in order to determine the fundamental spin–rotation–tensor components for the molecule (*12*).

EXPERIMENTAL DETAILS

(A) Laser Magnetic Resonance Measurements

Spectra were recorded using the water vapor laser-based LMR spectrometer described previously (*14*). The electric vector of the laser radiation was arranged to be parallel (π polarization) to the applied magnetic field. Magnetic flux density measurements were made using a Hall probe which was calibrated with an nmr gaussmeter period-

ically. Additionally, some of the stronger resonance lines were measured directly using an nmr gaussmeter and corrections made for the relative positions of the probe and the sample. The estimated uncertainties are $\pm 1 \times 10^{-4}$ T for the lines measured directly and ± 5–10×10^{-4} T otherwise.

The DO_2 radicals were formed in a flow system by mixing chlorine atoms, produced in a microwave discharge of a mixture of chlorine (4.8%) in helium, with a CD_3OD and O_2 mixture. The reactions producing the DO_2 are (*15*)

$$Cl + CD_3OD \rightarrow DCl + CD_2OD \quad (1)$$

and

$$CD_2OD + O_2 \rightarrow CD_2O + DO_2. \quad (2)$$

Typical flow conditions used were 0.048 cm^3 sec^{-1} (all flows are STP $\equiv$ 1 atm, 273 K) for the Cl_2/He mixture, 0.23 cm^3 sec^{-1} for O_2, and 0.02 cm^3 sec^{-1} for CD_3OD. Helium was added at a rate of 4.85 cm^3 sec^{-1} to stabilize the microwave discharge and an additional flow of 1.80 cm^3 sec^{-1} of helium was added to the flow tube as a carrier gas. The total pressure was 3.0 Torr in the reaction region. The products of the microwave discharge in the Cl_2/He mixture were reacted with the methanol and oxygen approximately 5 cm above the detection region of the spectrometer. On the basis of the measured rate constants for reactions (*1*) and (*2*) the DO_2 production was completed before detection. The reaction between chlorine atoms and CD_3OD produced less HO_2 than that with CH_3OD. This was probably due to the presence of other isotopic species, e.g., CH_3OH and CH_2DOH in the CH_3OD. The identity of DO_2 was supported by studies of its chemical behavior. For example, the observed resonance lines disappeared on the addition of excess NO since the reaction

$$DO_2 + NO \rightarrow OD + NO_2 \quad (3)$$

removes all the DO_2 (or HO_2). No transitions of OD were observed in π polarization at 118.6 μm, a result consistent with a previous LMR study at 118.8 μm (*16*). The lines from HO_2, O_2, OH, and NO at 118.6 μm are well known and were identified in separate experiments.

(B) Millimeter- and Submillimeter-Wave Measurements

The millimeter- and submillimeter-wave techniques used for the work at the Duke Microwave Laboratory have been described previously (*17, 18*). In this instance, the probe radiation was quasi-optically propagated through a free space absorption cell consisting of a pyrex pipe 2.2 m in length with an inner diameter of 10 cm. This cell was pumped with a 4-in. diffusion pump. Cylindrical electrodes were placed at each end of this tube and a glow discharge of length 1.5 m was established in a flowing mixture of O_2 and CH_3OD. Optimal DO_2 production was obtained with partial pressures of 35 mTorr of O_2 and 10 mTorr of CH_3OD and discharge currents of about 30 mA. Although this reaction was a convenient means of introducing the correct isotopic species into the reaction, it produced signals that were substantially weaker than observed in our earlier work on HO_2. For those experiments, the products of a microwave discharge in CF_4 were reacted with HOOH (*19*).

A coil was wrapped around the cell so that magnetic fields of up to about 100 G could be applied. The ability to investigate the Zeeman effect of observed lines was extremely important to help distinguish the lines of the magnetic DO_2 from the rich nonmagnetic spectra of the many species present in the glow discharge.

RESULTS

(A) Laser Magnetic Resonance Measurements

In Fig. 1, we show the observed laser magnetic resonance spectrum from 0–1.5 T taken in a fast scan using a 118.6-μm H_2O laser line at 2527.9531 GHz (*20*). The chemical evidence discussed in the previous section strongly suggested that all the

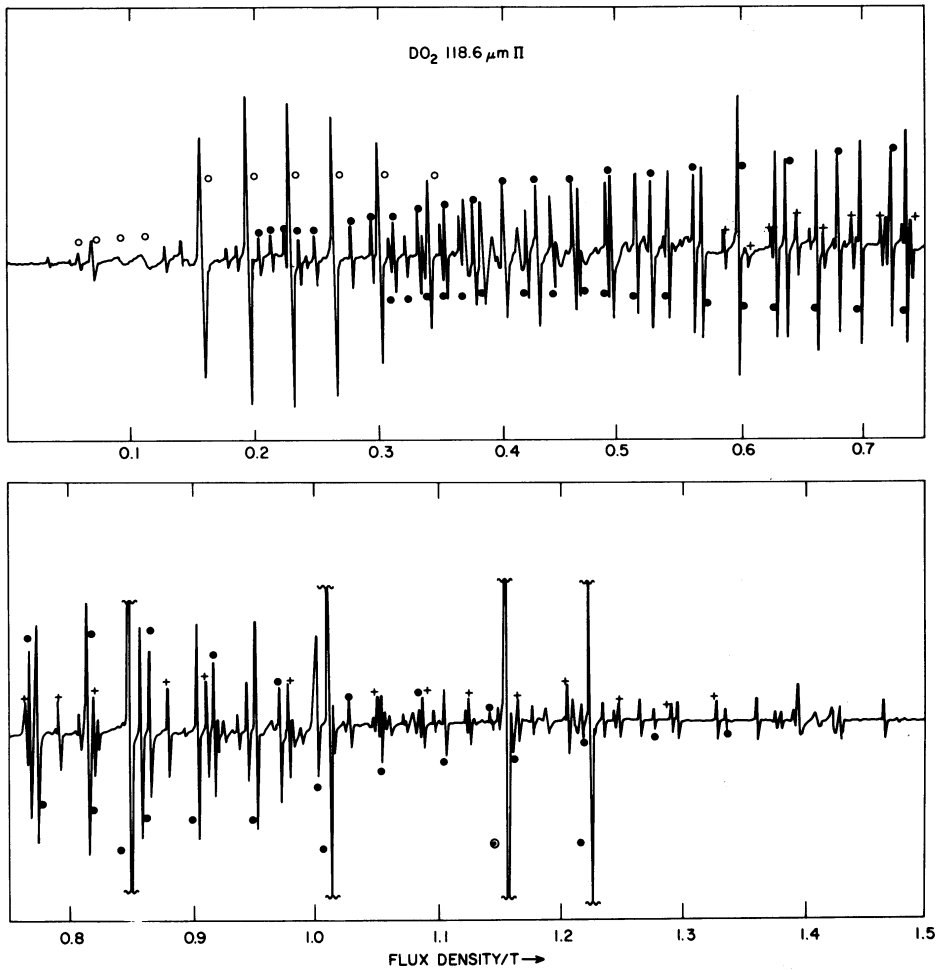

FIG. 1. Laser magnetic resonance spectrum of the DO_2 radical taken using the 118.6-μm water vapor laser line. The laser is polarized with the electric vector parallel to the applied magnetic field. The rotational transitions are identified by the following symbols: O, $20_{218} \leftarrow 19_{119}$; • (above resonance line), $17_{315} \leftarrow 15_{214}$; • (below resonance line), $16_{318} \leftarrow 15_{214}$; +, $18_{316} \leftarrow 17_{215}$; ⊕, $5_4 \leftarrow 4_3$; and ⊙, $6_4 \leftarrow 5_3$.

major resonance lines in the spectrum were attributable to DO_2. Some weak features could be assigned to HO_2 and O_2.

In order to assign the spectrum, the molecular parameters determined by Saito *et al.* (*9*) were used to calculate the rotational energy levels of the molecule and transitions with frequencies lying close to the laser frequency were picked out. The spin splittings of the levels involved were then used in an approximate calculation (*21*) of the magnetic field behavior for each transition and the observed and calculated Zeeman patterns matched in order to arrive at unambiguous assignments. Once all assignments had been made, the original predictions were refined and further assignments became straightforward. Ultimately, Zeeman components of eight rotational transitions were identified although two pairs of *K*-doublet transitions were unresolved. These were the $6_4 \leftarrow 5_3$ and $5_4 \leftarrow 4_3$; the *K* doubling in the 5_3 level is predicted to be about 2.5 MHz, hence its nonobservation is not surprising in view of the expected broadened linewidth of 6 MHz FWHM at 300 K at this frequency. The assigned resonances are given in Table I.

While this work was in progress we were informed by Dr. J. M. Brown[3] that a significant body of FIR LMR data existed that had been recorded at longer wavelengths and was thought to be due to DO_2. We have included a representative sample of this data in our analysis (see next section), and for completeness the assigned resonances are also given in Table I. We were not able to convincingly assign the spectrum recorded on the 394-μm HCOOH laser line (*10*) although most likely it is due to the transition $21_{219} \leftarrow 21_{120}$. The reason for the inability to decide on a unique assignment lies in the large number of incompletely resolved Zeeman components in the spectrum.

(B) Millimeter- and Submillimeter-Wave Measurements

These measurements were made at a time when the analysis of the LMR data in conjunction with the previously published data (*9, 10*) was well in hand. Consequently fairly good predictions of the expected frequencies could be made and this turned out to be necessary since the DO_2 lines were weaker than those of HO_2 previously studied (*6*), presumably due to a population dilution effect and the slightly less efficient chemistry employed. Additionally, many contaminant molecule lines were present in the chemical mixture and it was necessary to employ Zeeman effect measurements in order to unambiguously identify those lines due to DO_2. The measured frequencies are given in Table II. At these frequencies the Doppler and pressure broadened linewidths are greater than the hyperfine splittings due to the nuclear spin of deuterium, and hyperfine splitting was not observed in any of the lines. However, the effect of the unresolved hyperfine components is to shift the apparent position of the line center. Fortunately, the hyperfine parameters for DO_2 have been accurately determined from the work of Saito *et al.* (*9*) and these were used to estimate the hypothetical line position in the absence of nuclear hyperfine effects. These "corrected" frequencies ν_{FS} are also recorded in Table II; the changes are rather small as can be seen from the entries in the table.

[3] We are most grateful to J. M. Brown and H. E. Radford for providing us with this additional data.

TABLE I

Far-Infrared Laser Magnetic Resonance Data for DO_2

$6_{4} \leftarrow 5_{3}$ [a,b] Laser 2527.9531 GHz

2 MJ [c]	2 MJ	F [d]	F	FIELD Gauss	O-C FREQ [e] MHz	O-C FIELD [f] Gauss
11	11	2	1	11593	-14.4	-6

$5_{4} \leftarrow 4_{3}$ [b] Laser 2527.9531 GHz

2 MJ	2 MJ	F	F	FIELD Gauss	O-C FREQ MHz	O-C FIELD Gauss
-9	-9	2	1	8512	6.4	-2
-7	-7	2	1	10117	4.0	-2
-5	-5	2	1	12283	5.3	-3
-3	-3	2	1	15237	-0.3	0

$16_{313} \leftarrow 15_{214}$ Laser 2527.9531 GHz

2 MJ	2 MJ	F	F	FIELD Gauss	O-C FREQ MHz	O-C FIELD Gauss
-31	-31	2	1	3112	8.7	-3
-29	-29	2	1	3238	15.7	-6
-27	-27	2	1	3377	11.2	-4
-25	-25	2	1	3523	13.0	-5
-23	-23	2	1	3682	7.6	-3
-21	-21	2	1	3857	-10.3	4
-19	-19	2	1	4043	-25.9	11
-17	-17	2	1	4222	4.7	-2
-15	-15	2	1	4427	4.7	-2
-13	-13	2	1	4642	13.7	-6
-11	-11	2	1	4879	6.3	-3
-9	-9	2	1	5131	0.4	0
-7	-7	2	1	5392	10.5	-5
-5	-5	2	1	5673	13.9	-7
-3	-3	2	1	5973	14.3	-7
-1	-1	2	1	6296	4.3	-2
1	1	2	1	6628	15.0	-7
3	3	2	1	6983	17.1	-8
5	5	2	1	7364	5.1	-2
7	7	2	1	7757	9.3	-4
9	9	2	1	8179	-6.4	3
11	11	2	1	8605	12.4	-6
13	13	2	1	9069	-8.1	4
15	15	2	1	9537	6.9	-3
17	17	2	1	10023	27.3	-12

[a] Transition labelled by rotational quantum numbers $N'_{K'_a K'_c} \leftarrow N''_{K''_a K''_c}$.

[b] K doubling not resolved in these transitions.

[c] Twice the M_J value for the upper and lower state involved in the transition. $\Delta M_J = 0$ corresponds to π (parallel) polarization, $\Delta M_J = \pm 1$ corresponds to σ (perpendicular) polarization.

[d] F_1 and F_2 give the fine structure levels to which the M_J level correlates in zero field. F_1 corresponds to levels with $J = N + 1/2$ and F_2 to levels with $J = N - 1/2$.

[e] Observed minus calculated frequency using the parameters given in Tables III and V.

[f] Observed minus calculated field using the parameters given in Tables III and V.

TABLE I—*Continued*

2 MJ -- 2 MJ	F -- F	FIELD Gauss	O-C FREQ MHz	O-C FIELD Gauss
19 19	2 1	10540	23.6	-10
21 21	2 1	11090	-10.2	4
23 23	2 1	11636	13.9	-6
25 25	2 1	12220	-3.6	2
27 27	2 1	12802	36.7	-14
29 29	2 1	13404	83.0	-32

17 --- 16 Laser 2527.9531 GHz
315 214

2 MJ -- 2 MJ	F -- F	FIELD Gauss	O-C FREQ MHz	O-C FIELD Gauss
-29 -29	2 1	2056	-12.0	5
-27 -27	2 1	2156	-9.5	4
-25 -25	2 1	2260	3.9	-2
-23 -23	2 1	2374	14.9	-6
-21 -21	2 1	2504	12.4	-6
-17 -17	2 1	2800	5.8	-3
-15 -15	2 1	2965	8.4	-4
-13 -13	2 1	3147	6.2	-3
-11 -11	2 1	3341	11.7	-6
-9 -9	2 1	3557	7.2	-4
-7 -7	2 1	3787	10.7	-6
-5 -5	2 1	4043	1.0	-1
-3 -3	2 1	4311	6.4	-3
-1 -1	2 1	4602	7.3	-4
1 1	2 1	4913	10.5	-6
3 3	2 1	5248	9.0	-5
5 5	2 1	5600	16.2	-9
7 7	2 1	5973	24.6	-13
9 9	2 1	6380	9.3	-5
11 11	2 1	6798	13.0	-7
13 13	2 1	7243	4.4	-2
15 15	2 1	7700	12.0	-6
17 17	2 1	8179	15.4	-7
19 19	2 1	8680	13.3	-6
21 21	2 1	9205	0.1	0
23 23	2 1	9735	16.9	-8
25 25	2 1	10290	19.6	-8
27 27	2 1	10861	28.3	-12
29 29	2 1	11461	11.0	-4

18 --- 17 Laser 2527.9531 GHz
316 215

2 MJ -- 2 MJ	F -- F	FIELD Gauss	O-C FREQ MHz	O-C FIELD Gauss
-21 -21	1 2	5855	-34.7	-14
-19 -19	1 2	6059	-9.3	-4
-17 -17	1 2	6258	-18.5	-8
-15 -15	1 2	6465	-30.0	-12
-13 -13	1 2	6687	-27.5	-11
-11 -11	1 2	6911	-43.4	-18
-9 -9	1 2	7166	-8.5	-4
-7 -7	1 2	7410	-24.6	-10
-5 -5	1 2	7670	-27.2	-11
-3 -3	1 2	7942	-26.7	-11
-1 -1	1 2	8229	-16.4	-7
3 3	1 2	8825	-23.0	-10
5 5	1 2	9147	-9.8	-4
7 7	1 2	9470	-21.8	-9
9 9	1 2	9806	-30.7	-13
11 11	1 2	10161	-22.6	-9
13 13	1 2	10519	-35.9	-15
15 15	1 2	10895	-35.0	-14
17 17	1 2	11292	-12.5	-5
19 19	1 2	11685	-29.5	-12
21 21	1 2	12107	-5.3	-2
23 23	1 2	12520	-34.5	-14

TABLE I—*Continued*

20 --- 19 Laser 2527.9531 GHz
218 119

2 MJ -- 2 MJ	F -- F	FIELD Gauss	O-C FREQ MHz	O-C FIELD Gauss
27 27	2 1	582	-5.1	-4
25 25	2 1	701	-1.8	-2
25 25	2 1	1587	-0.7	1
27 27	2 1	1956	0.7	-1
29 29	2 1	2303	1.9	-2
31 31	2 1	2654	4.4	-4
33 33	2 1	3026	4.0	-3
35 35	2 1	3424	6.6	-5
37 37	2 1	3836	47.0	-30

3 --- 3 Laser 902.6301 GHz
2 1 1 2

2 MJ -- 2 MJ	F -- F	FIELD Gauss	O-C FREQ MHz	O-C FIELD Gauss
5 5	1 1	6951	-12.6	8
3 3	1 1	8548	-8.9	10
5 3	1 1	5768	-16.5	10
3 1	1 1	6972	-7.4	7

3 --- 3 Laser 903.8894 GHz
2 1 1 2

2 MJ -- 2 MJ	F -- F	FIELD Gauss	O-C FREQ MHz	O-C FIELD Gauss
5 5	1 1	7783	-3.7	3

4 --- 4 Laser 902.6301 GHz
2 2 1 3

2 MJ -- 2 MJ	F -- F	FIELD Gauss	O-C FREQ MHz	O-C FIELD Gauss
7 7	2 2	8615	16.2	13
7 7	1 1	8685	-12.4	10

4 --- 4 Laser 903.8894 GHz
2 2 1 3

2 MJ -- 2 MJ	F -- F	FIELD Gauss	O-C FREQ MHz	O-C FIELD Gauss
7 7	2 2	7644	6.6	5
7 7	1 1	9811	-0.3	0

5 --- 5 Laser 902.6301 GHz
2 3 1 4

2 MJ -- 2 MJ	F -- F	FIELD Gauss	O-C FREQ MHz	O-C FIELD Gauss
7 7	2 2	2587	14.7	13
5 5	2 2	2621	10.2	11
9 7	2 2	1979	12.5	11
7 5	2 2	1979	14.3	13
5 3	2 2	2034	14.0	15
3 1	2 2	2137	10.7	13
1 -1	2 2	2303	10.0	14
-1 -3	2 2	2550	6.6	11
-3 -5	2 2	2939	5.0	11
5 7	2 2	3418	13.3	14
3 5	2 2	3582	10.9	14
1 3	2 2	3917	6.6	11
-1 1	2 2	4510	6.5	14
-3 -1	2 2	5567	4.8	15
-5 -3	2 2	7755	2.9	16

TABLE I—*Continued*

5 2 3 --- 5 1 4 Laser 903.8894 GHz

2 MJ -- 2 MJ	F -- F	FIELD Gauss	O-C FREQ MHz	O-C FIELD Gauss
1 3	2 2	1446	0.8	3
-1 1	2 2	1475	0.7	3
3 5	2 2	1511	1.3	4
-3 -1	2 2	1611	0.5	2
-5 -3	2 2	1932	0.8	5

15 214 --- 14 213 Laser 903.8894 GHz

2 MJ -- 2 MJ	F -- F	FIELD Gauss	O-C FREQ MHz	O-C FIELD Gauss
29 29	1 1	780	-0.9	-6
27 27	1 1	830	-1.3	-10
25 25	1 1	892	-1.2	-10
23 23	1 1	962	-1.2	-11
21 21	1 1	1042	-1.3	-13
19 19	1 1	1139	-1.2	-13
17 17	1 1	1253	-1.2	-14
15 15	1 1	1391	-1.1	-14
13 13	1 1	1558	-1.2	-17
11 11	1 1	1769	-1.1	-18
9 9	1 1	2041	-0.9	-18
5 5	1 1	2875	-1.0	-27

22 221 --- 22 122 Laser 1281.6259 GHz

2 MJ -- 2 MJ	F -- F	FIELD Gauss	O-C FREQ MHz	O-C FIELD Gauss
45 45	1 1	2589	-7.7	-15
43 43	2 2	3065	-4.3	-8
41 41	2 2	3437	-3.5	-8
39 39	2 2	3805	-2.1	-5
37 37	2 2	4191	-1.0	-3
35 35	2 2	4607	-1.2	-4
33 33	2 2	5072	-0.7	-3
31 31	2 2	5600	0.0	0
29 29	2 2	6205	0.0	0
27 27	2 2	6915	0.1	0
25 25	2 2	7763	0.2	2
23 23	2 2	8795	0.3	3

ANALYSIS AND DISCUSSION

In order to extract the best possible set of molecular parameters for the DO_2 radical, the data given in Tables I and II were combined with the earlier millimeter-wave measurements reported by Saito *et al.* (*9*) and a representative sample of the LMR and EPR measurements reported by Barnes *et al.* (*10*). The millimeter-wave data (*9*) were corrected for the effects of nuclear hyperfine structure by explicitly subtracting the calculated hyperfine contributions from the frequencies using the hyperfine parameters given previously (*9*). As was the case for the millimeter-wave measurements discussed in the previous section, where hyperfine components were not resolved, an average calculated shift was applied with the individual components weighted according to their relative intensities. The appropriate effective Hamiltonian for DO_2 has been discussed by Bowater *et al.* (*22*), Watson (*23*), and Brown and Sears (*11*). A review of

TABLE II

Observed Millimeter-Wave Rotational Transitions in DO_2

Transition[a] $N'_{K_aK_c} \leftarrow N''_{K_aK_c}(J)$	ν_{OBS}[b] GHz	ν_{FS}[c] GHz	$\nu_{FS}-\nu_{CALC}$[d] MHz
6_{06} $5_{05}(F_2)$	362.121270	362.121232	0.001
6_{15} $5_{14}(F_1)$	371.287110	371.287136	-0.015
6_{15} $5_{14}(F_2)$	370.658488	370.658466	-0.153
6_{24} $5_{23}(F_2)$	361.339204	361.339166	-0.112
6_{25} $5_{24}(F_1)$	363.890893	363.890892	-0.084
6_{25} $5_{24}(F_2)$	360.644360	360.644321	-0.049
6_{33} $5_{32}(F_1)$	365.497943	365.497982	0.047
6_{33} $5_{32}(F_2)$	358.712770	358.712730	-0.137
6_{34} $5_{33}(F_1)$	365.493371	365.493411	0.090
6_{34} $5_{33}(F_2)$	358.708197	358.708157	0.100
6_4 5_4 (F_1)	367.058195	367.058232	0.144
6_4 5_4 (F_2)	356.290908	356.290873	0.024
7_{07} $6_{06}(F_1)$	421.955345	421.955370	-0.029
8_{08} $7_{17}(F_1)$	216.089908	216.089946	0.063
8_{08} $7_{17}(F_2)$	212.545859	212.545844	-0.046
7_{26} $8_{17}(F_1)$	375.499373	375.499378	0.115
8_{27} 9_{18} (F_1)	303.352729	303.352678	-0.067
8_{27} 9_{18} (F_2)	314.027549	314.027534	0.028
10_{10} 9_{19} (F_1)	355.904547	355.904555	-0.064
10_{10} 9_{19} (F_2)	353.407889	353.407885	0.017
10_{28} $11_{111}(F_1)$	350.110737	350.110722	0.040
10_{28} $11_{111}(F_2)$	360.789129	360.789148	-0.109
5_{14} 5_{05} (F_1)	324.067090[e]	324.067084	-0.629
5_{14} 5_{05} (F_2)	330.629783	330.629794	-0.051
6_{15} 5_{05} (F_1)	333.410162	333.410159	-0.025
6_{15} 6_{06} (F_2)	339.167233	339.167238	0.004
7_{16} 7_{07} (F_1)	344.375835	344.375822	-0.013
7_{16} 7_{07} (F_2)	349.577849	349.577853	-0.013
8_{17} 8_{08} (F_1)	357.092355	357.092354	0.000
8_{17} 8_{08} (F_2)	361.902939[e]	361.902938	-0.257
9_{18} 9_{09} (F_1)	371.685891	371.685882	-0.038
9_{18} 9_{09} (F_2)	376.220141	376.220153	-0.046
10_{19} $10_{010}(F_2)$	392.626997	392.626994	0.185

[a] Transition labelled by rotational quantum numbers and fine structure state (F_1 or F_2) where $F_1 \equiv J = N + 1/2$, $F_2 \equiv J = N - 1/2$ levels. All transitions obey the selection rule $\Delta N = \Delta J$.

[b] Observed frequency in GHz. Estimated accuracy is 0.030 MHz in most cases.

[c] Frequency corrected for unresolved hyperfine structure components using the hyperfine parameters given in reference (9).

[d] Frequency calculated using the parameters given in Table III.

[e] Transition given zero weight in the analysis.

TABLE II—*Continued*

Transition $N'_{K_aK_c} \leftarrow N''_{K_aK_c}$ (J)	ν_{OBS} GHz	ν_{FS} GHz	$\nu_{FS}-\nu_{CALC}$ MHz
11_{110} 11_{011} (F_2)	411.233980	411.233974	0.054
13_{112} 13_{113} (F_2)	258.460270	258.460204	-0.017
4_{14} 3_{13} (F_1)	236.856827	236.856914	0.042
4_{14} 3_{13} (F_2)	234.878866	234.878732	0.044
4_{13} 3_{12} (F_1)	248.107231	248.107289	-0.004
4_{13} 3_{12} (F_2)	246.323854	246.323794	-0.027
4_{04} 3_{03} (F_1)	241.554731	241.554801	0.029
4_{04} 3_{03} (F_2)	241.740117	241.740031	0.003
5_{33} 4_{32} (F_1)	306.031878	306.031932	0.185
5_{32} 4_{31} (F_1)	306.033254	306.033308	-0.155
5_{14} 4_{13} (F_1)	309.661832	309.661869	-0.021
5_{14} 4_{13} (F_2)	308.628779	308.628749	0.012

the form of the operator and the computational techniques used has been given previously (*24*). The effective operator is

$$H_{EFF} = H_R + H_{CD} + H_{SR} + H_{SRCD} + H_{HFS} + H_Z. \quad (4)$$

Here H_R and H_{CD} are the effective rotational and centrifugal distortion operators, H_{SR} and H_{SRCD} are the quadratic and quartic spin–rotation coupling terms, and H_{HFS} and H_Z the hyperfine coupling term and Zeeman interaction. The quadratic spin–rotation operator involves four determinable parameters in the present case (*11*) while the quartic term will in theory contain eight parameters for a planar unsymmetrical molecule such as DO_2. The exact form of this latter operator has not been established for such a case and we adopt the form appropriate for a molecule belonging to an orthorhombic point group on the basis that the neglected terms will have only a small effect on the eigenvalues of interest. Both rotational and spin–rotational operators were cast in the "*A*" reduced form (*23, 11*).

In the fit, the data were weighed according to the inverse square of the estimated experimental uncertainty. The uncertainty in the millimeter-wave measurements was estimated to be 30 kHz in the present work and Saito *et al.* (*9*) give estimated uncertainties for their measurements. The LMR data were estimated to be accurate to ±2 MHz on average. This is an approximation based on the uncertainty in setting the FIR laser to the peak of the gain curve and the average estimated field measurement error and several of the strong components of the 20_{218}–19_{119} transition were more accurately measured than this by direct reference to an nmr gaussmeter measurement. The EPR measurements of Barnes *et al.* (*10*) were estimated to have an uncertainty of 300 kHz. The data set included 180 transitions of which 77 were millimeter-wave measurements, the rest comprising a representative sample of the LMR and EPR measurements.

Preliminary fits indicated that the FIR LMR measurements made using the 433-μm formic acid laser line (*10*) were not in accord with the rest of the data, these being consistently calculated approximately 20 MHz too high. The laser line frequency is not thought to be in error; it has been used extensively to record the LMR spectrum of the formyl radical (*25*), and we suspect that there is an error in the magnetic flux density measurements in this case. These data were given zero weight in the final analysis. Several measurements in the millimeter-wave data set were deemed to deviate by unacceptable amounts from the calculated position based on the rest of the data. These are indicated in Table II and were also given zero weight in the final analysis. The overall quality of the fit can be judged from the observed − calculated columns of Tables I and II. While it is clear that there are some systematic trends in the FIR LMR data, we believe that these are mainly due to remaining small systematic errors which remain in the field measurements. The residuals for the millimeter-wave measurements are very satisfactory; however, the overall standard deviation of the fit was a factor of three higher than expected on the basis of the estimated experimental uncertainties, and no combination of parameters could be found which reduced it further.

The parameters determined in the analysis are given in Tables III–V. The rotational and quartic centrifugal distortion parameters were all well determined, however, it was not possible to determine all of the expected sextic centrifugal distortion constants as might be expected for the limited data set; we believe that the parameters determined here can be used to reliably calculate the rotational energy levels with $N \leqslant 22$ and $K \leqslant 4$ to within a few MHz. Since the rotational Hamiltonian is fairly convergent for

TABLE III

Molecular Parameters for $\tilde{X}^2A''$ DO_2[a]

A	335.59994(3)	ϵ_{aa} = -27.145205(86)[c]
B	31.656479(13)	ϵ_{bb} = -0.391615(93)
C	28.810803(13)	ϵ_{cc} = 0.006802(93)
		$\lvert\epsilon_{ab} + \epsilon_{ba}\rvert$ = 0.0786(28)
$10^4\ \Delta_N$	0.93954(30)	
$10^2\ \Delta_{NK}$	0.225799(47)	$10^2\ \Delta_K^S$ = 0.6587(33)
Δ_K	0.0402016(99)	$10^3(\Delta_{NK}^S + \Delta_{KN}^S)$ = 0.512(23)
$10^5\ \delta_N$	0.85390(57)	$10^3\ \Delta_{NK}^S$ = -0.393(52)
$10^2\ \delta_K$	0.14649(63)	$10^6\ \delta_K^S$ = 0.23(13)
$10^7\ \Phi_{NK}$[b]	0.328(42)	
$10^4\ \Phi_K$	0.248(13)	

[a] Units are GHz. The numbers in parentheses are the estimated variances in units of the last quoted significant figure.

[b] All other sextic and higher centrifugal distortion constant constrained to zero.

[c] Determinable spin-rotation tensor components (see text).

TABLE IV

Spin–Rotation Parameters for HO_2 and DO_2

Quantity	Observed GHz	Calculated-1[b] GHz	Calculated-2[c] GHz
(i) For HO_2			
$\tilde{\epsilon}_{bb}$	-0.422755(60)[a]	-0.42530	-0.42458
$(\tilde{\epsilon}_{ab}+\tilde{\epsilon}_{ba})$	-0.3879(3)[a]	-0.3509	-0.3485
$\tilde{\epsilon}_{aa}$	-49.57141(14)[a]	-49.5885	-49.5896
ϵ_{bb}	----	-0.4228(89)	-0.4225(95)
ϵ_{ba}	----	-0.600(202)	-0.556(217)
ϵ_{ab}	----	7.81(3.67)	7.02(3.95)
ϵ_{aa}	----	-49.564(34)	-49.570(35)
(ii) For DO_2			
$\tilde{\epsilon}_{bb}$	-0.391615(93)[d]	-0.3855	-0.3873
$\lvert\tilde{\epsilon}_{ab}+\tilde{\epsilon}_{ba}\rvert$	0.0786(28)[d]	0.2409	0.1729
$\tilde{\epsilon}_{aa}$	-27.145205(86)[d]	-27.1335	-27.2317

[a] Ref. 6. Numbers in parentheses are one standard deviation of the least squares fits.

[b] Calculated assuming $\tilde{\epsilon}_{ab} + \tilde{\epsilon}_{ba}$ for DO_2 is positive.

[c] Calculated assuming $\tilde{\epsilon}_{ab} + \tilde{\epsilon}_{ba}$ for DO_2 is negative.

[d] Present work.

DO_2, calculated levels slightly outside these limits should also be fairly reliable. We will now consider specific aspects of the fitting in detail.

(i) Spin–Rotation Parameters

The quadratic spin–rotation Hamiltonian contains four determinable parameters for a molecule such as DO_2, usually taken as the three diagonal tensor components and the sum of the symmetry-allowed off-diagonal components $|\tilde{\epsilon}_{ba} + \tilde{\epsilon}_{ab}|$ (*11*). It is not possible to determine the sign of this quantity from experimental data since its matrix elements have no first-order effect on the eigenvalues. The four determinable quantities are linear combinations of the five symmetry-allowed nonzero tensor components as shown by Brown and Sears (*11*). It is these five parameters that may be related to the spin–orbit and Coriolis mixing of excited electronic states by (*26*)

TABLE V

Zeeman Parameters for $\tilde{X}^2A''$ DO_2

	Experiment[a]	Theory
(i) Spin Zeeman Interaction		
g_s^{aa}	2.04245(27)	2.04276[b]
g_s^{bb}	2.00795(23)	2.00850[b]
g_s^{cc}	2.00129(23)	2.00220[b]
(ii) Rotational Zeeman Interaction		
g_r^{aa}	-0.00514(11)	-0.00600[c]
g_r^{bb}	-0.000304(91)	-0.00009[c]
g_r^{cc}	-0.000224(91)	-1.33×10^{-6} [c]

[a] This work.

[b] Reference 37.

[c] Reference 7. Electronic contributions only to the rotational g-factors. The nuclear contribution is likely to be positive and of the order of 10^{-4} Bohr Magnetons.

$$\epsilon_{ab} = -4 \sum_n{}' \langle 0|B_\alpha L_\alpha|n\rangle\langle n|\xi_\beta L_\beta|0\rangle/(E_0 - E_n). \tag{5}$$

Here B_α is the α diagonal component of the inverse inertial tensor in the axis system while ξ_β is the β component of the spin–orbit operator. Brown *et al.* (*12*) showed how the $\epsilon_{\alpha\beta}$ parameters may be determined by combining the values obtained for the transformed parameters appearing in the effective Hamiltonian for two isotopic variants of the same species.

The theory developed strictly applies only to the equilibrium values of the parameters and at an early stage in the analysis an attempt was made to calculate the equilibrium spin–rotation tensor components for HO_2 and DO_2. There is now information on the diagonal tensor components in excited vibrational states in the literature (*27–31*) and the equilibrium structure of the radical has been experimentally determined. However, the accuracy of the determination of the vibrationally excited state spin–rotation tensor components is in all cases lower than the corresponding ground state parameters and these errors naturally carry over to the estimated equilibrium parameters.

A further problem is that the transformation used to generate the standard form (*11*) spin–rotation Hamiltonian introduces corrections to the quadratic spin–rotation parameters which are of the order of the quartic ones in an analogous way to that arising in a pure rotational Hamiltonian (*32*). In contrast to the rotational operator, these have not been evaluated in the spin–rotation case. For these reasons and following several trial fits, it was decided to consistently use the r_0 parameters and to neglect the effects of zero point vibration. Since it is clear (*27–31*) that the zero point correction to ϵ_{aa} in HO_2 for example is of the order of 1–2 GHz, this is probably the least secure

feature of the following analysis. With this provision, we combine the spin–rotation parameters for DO_2 derived in the present work with those for HO_2 (*6*) and attempt to determine the fundamental spin–rotation constants for the HO_2 and DO_2 molecules. In this respect the HO_2/DO_2 system provides a unique opportunity to test the applicability of the relationships derived by Brown *et al.* (*12*) since HO_2 and DO_2 are the best characterized examples of free radicals possessing C_s symmetry. This is the case where the theory is likely to be of the most value.

The calculation proceeds in the way described previously (*12*). The input consists of the six determinable in-plane components of the spin–rotation tensor ($\tilde{\epsilon}_{aa}$, $|\tilde{\epsilon}_{ab} + \tilde{\epsilon}_{ba}|$, and $\tilde{\epsilon}_{bb}$) for HO_2 (*6*) and DO_2 weighted according to their experimental uncertainties. These are used to determine the four fundamental spin–rotation constants for HO_2 (ϵ_{aa}, ϵ_{ab}, ϵ_{ba}, and ϵ_{bb}) which are related to the corresponding quantities for DO_2 by the isotope relations (*12*). Although only the magnitude of the off-diagonal component of the spin–rotation tensor can be determined from a fit to experimental data, the negative values determined for the in-plane components ϵ_{aa} and ϵ_{bb} suggested that it was likely to be negative also. However, all possibilities were investigated in various fits and a slightly lower standard deviation resulted when $(\tilde{\epsilon}_{ab} + \tilde{\epsilon}_{bc})$ for DO_2 was assumed to be positive. The results of two fits, the first with both ($\tilde{\epsilon}_{ab}$ and $\tilde{\epsilon}_{ba}$) for HO_2 and DO_2 positive and the second with $(\tilde{\epsilon}_{ab} + \tilde{\epsilon}_{ba})$ for DO_2 negative are summarized in Table IV. Fits with the same quantity for HO_2 set to a positive value invariably had a factor of 5 higher standard deviation.

The most interesting result of the present fits is the fact that the parameter ϵ_{ab} for HO_2 is determined to be a positive quantity. This result holds when $(\tilde{\epsilon}_{ab} + \tilde{\epsilon}_{ba})$ for DO_2 is taken to be a positive or a negative quantity. Whereas the value for ϵ_{aa} can be understood in terms of mixing of the $\tilde{A}^2A'$ state alone (*7*), this is certainly not the case for the other components. In order to gain further insight into the spin–orbit mixing of the various excited electronic states, it is necessary to have reliable estimates of both the spin–orbit integrals and the positions of the lowest few excited states of the molecule. From an experimental standpoint, the only state apart from the ground state at all well characterized is the $\tilde{A}^2A'$ (*33, 34*) from the $\tilde{A} \rightarrow \tilde{X}$ emission spectrum in the near infrared. Although some low-resolution data are available from UV absorption work on higher states (*35, 36*), the spectra are broad and not well resolved. Several high-quality ab initio calculations have recently been performed (*37, 38*) but in no case do the authors evaluate the spin–orbit integrals from the wavefunctions. It would be interesting if these quantities were available in order that the relative importance of the various possible contaminating states could be assessed.

From an experimental standpoint, improved measurements of the spin–rotation tensor components in excited vibrational states of the molecule would enable a better estimate of the zero point corrections necessary for a rigorous test of the theory. Unfortunately, the parameter where zero point corrections are likely to be most important, $|\tilde{\epsilon}_{ab} + \tilde{\epsilon}_{ba}|$, is the most difficult to measure, having only very small effects on a few specific levels.

The data have allowed a reliable determination of some of the quartic spin–rotation parameters for the molecule. Brown and Sears (*39*) showed how these arise due to the dependence of the inertial tensor and spin–rotation tensor on the vibrational normal coordinates. We can use their results to estimate the expected values for the dominant

quartic spin–rotation terms based on the quadratic parameters and the quartic centrifugal distortion constants determined here. We find the theoretical values are $\Delta_K^S = 0.65 \times 10^{-2}$, $\Delta_{NK}^S + \Delta_{KN}^S = 0.41 \times 10^{-3}$, and $\Delta_{NK}^S = 0.36 \times 10^{-3}$ GHz, so that there is good agreement in the first two cases but not for Δ_{NK}^S. Previously, the relationships derived by Brown and Sears have been found to give reasonable estimate of Δ_K^S (*7, 11, 39*), however, estimates for the smaller parameters are often unreliable. The comparison is complicated in all cases, however, by the inability to determine all of the quartic spin–rotation parameters accurately due to insufficient data.

(ii) Zeeman Parameters

There are two major contributions in the Zeeman Hamiltonian for DO_2, the spin Zeeman term, arising from the interaction of the unpaired electron spin angular momentum and the external magnetic field, which dominates, and the rotational Zeeman operator arising due to the interaction between the angular momentum of molecular rotation and the magnetic field. Each operator includes a second-rank g-factor tensor and the diagonal elements of both of them have been determined. For a light molecule such as DO_2, these quantities can be estimated from theoretical arguments, and Table V compares the results obtained experimentally with the theoretical predictions (*40, 7*). The spin Zeeman g-factors can be estimated from Curl's relationship (*40*) which has been found to be rather reliable for several light triatomic free radicals (*7, 39, 41*), and preliminary fits were attempted where the spin g-factors were held at their theoretical values. This procedure resulted in systematic residuals in the calculated magnetic flux densities, and the final resulting parameters differ slightly but significantly from the Curl's relationship values. To quantify this discrepancy more reliably requires more precise field measurement than was used in the present work. Additionally, the effect of the off-diagonal components g^{ab} and g^{ba} have been ignored. During the analysis, the effect of introducing these terms was investigated, and it was found that they introduced negligible changes in the calculated frequencies when the field measurement accuracy was taken into account, however, it is possible that the values for the diagonal components determined are influenced to a small extent by the neglect of the off-diagonal terms.

The theoretical estimates of the rotational g-factors rely on rather less soundly based arguments than is the case for the spin Zeeman g-factors. However, where it has been tested, the simple relationship derived by Barnes *et al.* (*7*) has been found to be fairly reliable. In the present case, the estimate for g_r^{aa} is seen to be very good; however, the experimentally determined g_r^{bb} and g_r^{cc} components are of considerably larger magnitude than is expected on theoretical grounds. In contrast, Barnes *et al.* (*7*) found reasonable agreement in the case of HO_2, and it is possible that in the present work, these parameters are effectively mimicking the effects of neglected terms, such as higher centrifugal distortion parameters, in the zero field Hamiltonian.

SUMMARY AND CONCLUSIONS

We have reported the measurement of many new rotational transitions in the deuteroperoxyl radical using the complementary techniques of FIR LMR and millimeter-

wave absorption spectroscopy. The data have been analyzed in conjunction with all previously published high-resolution data relating to the ground state of the molecule in order to estimate a rather complete set of molecular parameters for this state. Particular attention has been paid to the details of the spin–rotation interaction tensor components and by analyzing the present results together with the analogous ones for HO_2, we have estimated values for all of the symmetry-allowed spin–rotation tensor components for the HO_2/DO_2 system. This is the first case for which this has been possible, and it has yielded the surprising result that the two off-diagonal components of the tensor have the opposite signs. Accurate ab initio calculations of the spin–orbit matrix elements between the ground and lowest few excited electronic states are necessary in order to explain or rationalize this result in detail.

The least satisfactory aspect of the spin–rotation analysis is the use of zero point rather than equilibrium parameters, and further experimental work is needed before reliable estimates of the zero point contributions to the fine structure parameters can be assessed. Very recently, a high-resolution infrared spectrum of the hydroperoxyl radical has been obtained by standard Fourier transform infrared spectroscopy (*42*). Although the ultimate resolution of this technique is not as high as the methods employed in the present study, large amounts of data can be obtained in a comparatively short time, and it is likely that improved determinations of the spin–rotation tensor components in excited vibrational levels will be forthcoming.

One disconcerting aspect discovered in the present work was the difficulty in reliably determining the off-diagonal component of the spin–rotation tensor from the LMR data alone. Although many of the rotational levels included in the LMR data set are subject to shifts induced by this term in the Hamiltonian, it was only possible to estimate a value for this parameter with acceptably small standard deviation after the additional millimeter-wave measurements had been made. At first, we believed that this was due to a correlation problem involving $|\tilde{\epsilon}_{ab} + \tilde{\epsilon}_{ba}|$ and $|g_{ab}|$, which of course does not arise in the zero field measurements. Subsequently, it was determined that for all reasonable values of g_{ab}, estimated changes in the calculated magnetic fields in the magnetic resonance data set were small. We now feel that our inability to determine $|\tilde{\epsilon}_{ab} + \tilde{\epsilon}_{ba}|$ accurately from the magnetic resonance data was solely due to their lower accuracy compared to the millimeter-wave measurements. The situation would be helped by improved accuracy in the experimental magnetic flux densities, a solution which is in principle straightforward but in practice rather time consuming. Nonetheless, this study points out the desirability of doing this if one is to take full advantage of the resolution and sensitivity of the LMR experiment.

ACKNOWLEDGMENTS

This work was supported in part by the Chemical Manufacturers Association Technical Panel on Fluorocarbon Research and NOAA as part of the National Acid precipitation Assessment Program. We thank K. Evenson, D. Jennings, J. Brown, and H. Bandow for their support and encouragement during the course of this work, and S. Saito for providing us with unpublished calculations allowing us to check our computer codes. Research carried out at Brookhaven National Laboratory was under Contract DE-AC02-76CH00016 with the U.S. Department of Energy and supported by its Office of Basic Energy Sciences.

RECEIVED: November 25, 1985

REFERENCES

1. H. E. RADFORD, K. M. EVENSON, AND C. J. HOWARD, *J. Chem. Phys.* **60,** 3178–3183 (1974).
2. J. T. HOUGEN, H. E. RADFORD, K. M. EVENSON, AND C. J. HOWARD, *J. Mol. Spectrosc.* **56,** 210–228 (1975).
3. Y. BEERS AND C. J. HOWARD, *J. Chem. Phys.* **63,** 4212–4216 (1975).
4. S. SAITO, *J. Mol. Spectrosc.* **65,** 229–238 (1977).
5. S. SAITO AND C. MATSUMURA, *J. Mol. Spectrosc.* **80,** 34–40 (1980).
6. A. CHARO AND F. C. DE LUCIA, *J. Mol. Spectrosc.* **94,** 426–436 (1982).
7. C. A. BARNES, J. M. BROWN, A. CARRINGTON, J. PINKSTONE, T. J. SEARS, AND P. J. THISTLETHWAITE, *J. Mol. Spectrosc.* **72,** 86–101 (1978).
8. Y. BEERS AND C. J. HOWARD, *J. Chem. Phys.* **64,** 1541–1543 (1976).
9. S. SAITO, Y. ENDO, AND E. HIROTA, *J. Mol. Spectrosc.* **98,** 138–145 (1983).
10. C. E. BARNES, J. M. BROWN, AND H. E. RADFORD, *J. Mol. Spectrosc.* **84,** 179–196 (1980).
11. J. M. BROWN AND T. J. SEARS, *J. Mol. Spectrosc.* **75,** 111–133 (1979).
12. J. M. BROWN, T. J. SEARS, AND J. K. G. WATSON, *Mol. Phys.* **41,** 173–182 (1980).
13. D. L. BAULCH, R. A. COX, R. F. HAMPSON, JR., J. A. KERR, J. TROE, AND R. T. WATSON, *J. Phys. Chem. Ref. Data* **9,** 295–469 (1980).
14. C. J. HOWARD AND K. M. EVENSON, *J. Chem. Phys.* **61,** 1943–1952 (1974).
15. H. E. RADFORD, *Chem. Phys. Lett.* **71,** 195–197 (1980).
16. J. S. GEIGER, D. R. SMITH, AND J. D. BONNETT, *Chem. Phys. Lett.* **70,** 600–604 (1980).
17. F. C. DE LUCIA, *in* "Molecular Spectroscopy: Modern Research" (K. Narahari Rao, Ed.), Academic Press, New York, 1976.
18. P. HELMINGER, J. K. MESSER, AND F. C. DE LUCIA, *Appl. Phys. Lett.* **42,** 309–310 (1983).
19. A. CHARO AND F. C. DE LUCIA, *J. Mol. Spectrosc.* **94,** 426–436 (1982).
20. D. J. E. KNIGHT, unpublished results.
21. T. J. SEARS, P. R. BUNKER, A. R. W. MCKELLAR, K. M. EVENSON, D. A. JENNINGS, AND J. M. BROWN, *J. Chem. Phys.* **77,** 5348–5362 (1982).
22. I. C. BOWATER, J. M. BROWN, AND A. CARRINGTON, *Proc. R. Soc. London Ser. A* **333,** 265–288 (1973).
23. J. K. G. WATSON, *in* "Vibrational Spectra and Structure" (J. R. Durig, Ed.), Vol. 6, Elsevier, Amsterdam, 1977.
24. T. J. SEARS, *Comp. Phys. Rep.* **2,** 1–32 (1984).
25. J. M. BROWN, H. E. RADFORD, AND T. J. SEARS, in press.
26. J. H. VAN VLECK, *Rev. Mod. Phys.* **23,** 213–227 (1951).
27. A. R. W. MCKELLAR, *Faraday Discuss. Chem. Soc.* **71,** 63–76 (1981).
28. K. NAGAI, Y. ENDO, AND E. HIROTA, *J. Mol. Spectrosc.* **89,** 520–527 (1981).
29. C. YAMADA, Y. ENDO, AND E. HIROTA, *J. Chem. Phys.* **78,** 4379–4384 (1983).
30. K. LUBIC, T. AMANO, H. NEHARA, K. KAWAGUCHI, AND E. HIROTA, *J. Chem. Phys.* **81,** 4826–4831 (1984).
31. H. UEHARA, K. KAWAGUCHI, AND E. HIROTA, *J. Chem. Phys.* **83,** 5479–5485 (1985).
32. D. KIVELSON AND E. B. WILSON, *J. Chem. Phys.* **20,** 1575–1579 (1952).
33. P. A. FREEDMAN AND W. J. JONES, *J. Chem. Soc. Faraday. Trans. II* **72,** 207–215 (1976).
34. R. P. TUCKETT, P. A. FREEDMAN, AND W. J. JONES, *Mol. Phys.* **37,** 379–403 (1979).
35. T. T. PAUKERT AND H. S. JOHNSTON, *J. Chem. Phys.* **56,** 2824–2838 (1972).
36. C. J. HOCHANADEL, J. A. GHORMLEY, AND P. J. OGREN, *J. Chem. Phys.* **56,** 4426–4432 (1972).
37. S. R. LANGHOFF AND R. L. JAFFE, *J. Chem. Phys.* **71,** 1475–1485 (1979).
38. G. J. VAZQUEZ, S. D. PEYERIMHOFF, AND R. J. BEUNKER, *Chem. Phys.* **99,** 239–258 (1985).
39. J. M. BROWN AND T. J. SEARS, *Mol. Phys.* **34,** 1595–1610 (1977).
40. R. F. CURL, JR., *Mol. Phys.* **9,** 585–597 (1965).
41. K. KAWAGUCHI, C. YAMADA, E. HIROTA, J. M. BROWN, J. BUTTENSHAW, C. R. PARENT, AND T. J. SEARS, *J. Mol. Spectrosc.* **81,** 61–72 (1980).
42. C. J. HOWARD, "XVII International Symposium on Free Radicals," Granby, Colo., 1985.